10

Morse Theoretic Reconstructions

In this chapter we describe algorithms for surface reconstruction that are based on Morse Theory, a well-known topic in differential topology. We describe two algorithms which are similar in principle though are different in details. We will not go over the proofs of geometric and topological guarantees of these algorithms as in previous chapters. Instead, we will emphasize their novel use of the Voronoi and Delaunay diagrams with Morse theoretic interpretations. In practice, for reasonably dense samples, these algorithms produce comparable results with other provable algorithms.

10.1 Morse Functions and Flows

Let $h\colon \mathbb{R}^3 \to \mathbb{R}$ be a smooth function. The smoothness means that h is continuous and infinitely often differentiable. The gradient ∇h of h at a point x is given by

$$\nabla h(x) = \left(\frac{\partial h}{\partial x_1}(x) \;\; \frac{\partial h}{\partial x_2}(x) \;\; \frac{\partial h}{\partial x_3}(x) \right).$$

This gradient induces a vector field $v\colon \mathbb{R}^3 \to \mathbb{R}^3$ where $v(x) = \nabla h(x)$. This vector field is smooth since h is so. A point x is *critical* if $\nabla h(x) = (0, 0, 0)$. The *Hessian* of h at x is the three by three matrix

$$\begin{pmatrix} \frac{\partial^2 h}{\partial x_1^2} & \frac{\partial^2 h}{\partial x_1 \partial x_2} & \frac{\partial^2 h}{\partial x_1 \partial x_3} \\ \frac{\partial^2 h}{\partial x_2 \partial x_1} & \frac{\partial^2 h}{\partial x_2^2} & \frac{\partial^2 h}{\partial x_2 \partial x_3} \\ \frac{\partial^2 h}{\partial x_3 \delta x_1} & \frac{\partial^2 h}{\partial x_3 \partial x_2} & \frac{\partial^2 h}{\partial x_3^2} \end{pmatrix} \text{ evaluated at } x.$$

A critical point of h is *nondegenerate* if the Hessian at that point is not singular. The function h is called a nondegenerate Morse function if all its critical points are nondegenerate. Nondegenerate critical points are necessarily isolated. They

are characterized by the celebrated Morse Lemma which says that each critical point x has a local coordinate system with the origin at x so that

$$h(y) = h(x = 0) \pm x_1^2 \pm x_2^2 \pm x_3^2$$

for all $y = (x_1, x_2, x_3)$ in a neighborhood of x. The number of minus signs in the above expression is the *index* of x. The critical points of index 0 are the local minima, and the critical points of index 3 are the local maxima of h. The rest of the critical points are saddle points which may have index 1 or 2.

The gradient vector field v gives rise to an ordinary differential equation

$$\frac{d}{dt}\phi(t, x) = v(\phi(t, x)).$$

The solution of the equation is a map $\phi : \mathbb{R} \times \mathbb{R}^3 \to \mathbb{R}^3$ which has the following two properties:

(i) $\phi(0, x) = x$
(ii) $\phi(t, \phi(s, x)) = \phi((t + s), x)$.

The function ϕ is called a *flow* on $\mathbb{R}^3$. Its first parameter can be thought of as time and the mapping itself tells how points in $\mathbb{R}^3$ move in time with the vector field v. The first property says that points have not moved yet at time zero. The second property says that a point after time $t + s$ moves to a position where $\phi(s, x)$ moves after time t. The points which do not move at all, that is, where $\phi(t, x) = x$ for all $t \in \mathbb{R}$ are called the *fixed points* of ϕ. It turns out that the critical points of h are the fixed points of ϕ.

An embedding of the real line $\mathbb{R}$ into $\mathbb{R}^3$ can be obtained from ϕ for each x by keeping the second parameter fixed to x. The curve $\phi_x : \mathbb{R} \to \mathbb{R}^3$ where $\phi_x(t) = \phi(t, x)$ is called the *flow curve* of x. The flow curve ϕ_x describes how the point x moves in time which could be negative. This motion always follows the steepest ascent of the function h, that is the direction in which h increases the most. In other words, the flow curves are the integral curves of the gradient vector field v (see Figure 10.1). A natural orientation can be imposed on the flow curves with increasing value of h. The flow curves are open and as such do not have endpoints. However, if a flow curve is not flowing into infinity, its closure will have two critical points at the ends, one where it originates, the other where it terminates. The first one is called the *origin* and the second one is called the *destination* of the flow curve. To be uniform, we introduce a critical point p_∞ at infinity so that all flow curves have an origin and a destination.

Let $C(h)$ be the set of critical points of h. For a critical point $c \in C(h)$ we are interested in the points that are flowing into c. This means it is the set of points covered by the flow curves that have c as their destination. This motivates the

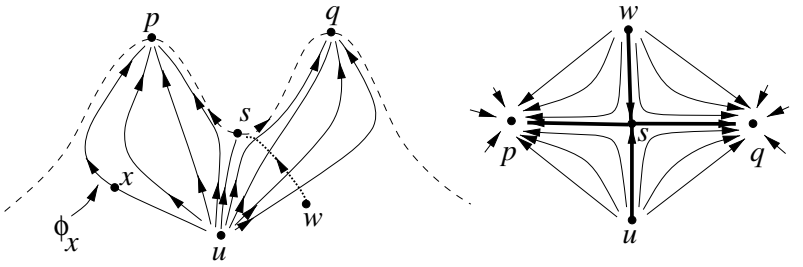

Figure 10.1. Flow curves drawn on the graph of a function from $\mathbb{R}^2$ to $\mathbb{R}$. The peaks of the two humps correspond to two maxima p and q. The point s corresponds to a saddle and u, w correspond to minima. The flow curve ϕ_x originates at u and terminates at p. On right the flow curves are drawn on the domain $\mathbb{R}^2$. The stable and unstable manifolds of s are drawn with thicker curves, $S(s) = us \cup ws$, $U(s) = ps \cup qs$.

definition of *stable manifold* of c as

$$S(c) = \{c\} \cup \{y \in \mathbb{R}^3 \mid c \text{ is the destination of } \phi_y\}.$$

If c is a minimum, that is, its index is 0, then $S(c) = \{c\}$ since no flow curve has c as a destination. If the index of c is $j > 0$, the stable manifold $S(c)$ consists of c and a $(j-1)$-dimensional sphere of flow curves which means $S(c)$ is j-dimensional. For all c, $S(c)$ is the image of an injective map from $\mathbb{R}^j$ to $\mathbb{R}^3$. It is homeomorphic to $\mathbb{R}^j$ although its closure may not be homeomorphic to a closed ball $\mathbb{B}^j$. This exception can happen only if the closure of two flow curves coming into c share the starting point. The stable manifold $S(p_\infty)$ is the image of an injective map from the punctured three-dimensional sphere, $\mathbb{R}^3 \setminus \{0\}$, to $\mathbb{R}^3$. The stable manifolds are mutually disjoint open sets and they cover the entire $\mathbb{R}^3$, that is,

(i) $S(c) \cap S(c') = \emptyset$ for any $c \neq c'$,
(ii) $\bigcup_{c \in C(h)} S(c) = \mathbb{R}^3$.

Similar to the stable manifolds, one may define *unstable manifolds* for the critical points. These are the spaces of flow curves that originates at the critical points. Formally, the unstable manifold $U(c)$ for a critical point $c \in C(h)$ is given by

$$U(c) = \{c\} \cup \{y \in \mathbb{R}^3 \mid c \text{ is the origin of } \phi_y\}.$$

The dimensions of the stable and unstable manifolds add up to the dimension of the domain, that is, $U(c)$ is $(3-j)$-dimensional if c has index j. This means a minimum has an unstable manifold of dimension 3 and a maximum has an

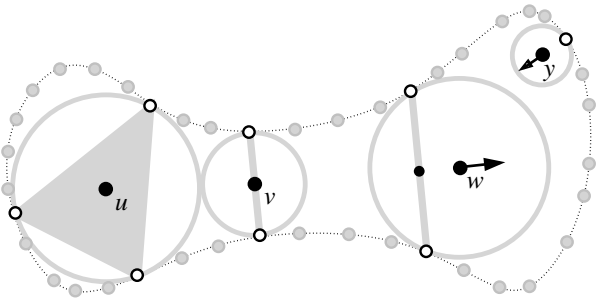

Figure 10.2. In this example the point set P is a sample from a curve $\Sigma \subset \mathbb{R}^2$. The sets $A(x)$ are shown with hollow circles for four points $x = u, v, w, y \in \mathbb{R}^2$. The convex hulls of $A(x)$ are lightly shaded. The driver of the point w is the smaller black circle. The driver of the point y is the single point in $A(y)$. The points u and v are critical since they are contained in $H(u)$ and $H(v)$ respectively. The points w and y are regular. The direction of steepest ascent of the distance function at w and y is indicated by an arrow.

unstable manifold of dimension 0. Similar to the stable manifolds, we have the following properties for the unstable ones:

(i) $U(c) \cap U(c') = \emptyset$ for any $c \neq c'$,
(ii) $\bigcup_{c \in C(h)} U(c) = \mathbb{R}^3$.

10.2 Discretization

In surface reconstruction from a point sample $P \subset \Sigma$, we have a distance function $d : \mathbb{R}^3 \to \mathbb{R}$ where $d(x)$ is the squared distance of x to the nearest point in P, that is, $d(x) = d(x, P)^2$. Unfortunately, we cannot use the setup developed for the smooth functions since d is not necessarily smooth. In particular, d is not smooth at the Voronoi facets, edges, and vertices of Vor P though it remains smooth in the interior of each Voronoi cell. Therefore, we cannot apply the theory of ordinary differential equations to get the flow curves and the associated stable manifolds. Nevertheless, there is a unique direction of steepest ascent of d at each point of $\mathbb{R}^3$ except at the critical points of d. This is what is used to define a vector field and the associated flow curves.

10.2.1 Vector Field

We need to determine the direction of the steepest ascent of d as well as its critical points. The following definitions are helpful to determine them. See Figure 10.2 for illustrations of the terms.

Definition 10.1. *For every point $x \in \mathbb{R}^3$, let $A(x)$ be the set of points in P with minimum distance to x, that is, $A(x) = \text{argmin}_{p \in P} \| p - x \|$. Let $H(x)$ be the convex hull of $A(x)$. The point x is* critical *if $x \in H(x)$ and is* regular *otherwise.*

Definition 10.2. *For any point $x \in \mathbb{R}^3$, let $r(x)$ be the point in $H(x)$ closest to x. The point $r(x)$ is called the* driver *of x.*

The following lemma plays a key role in defining a flow from d. To keep the discussion simple we assume that no four points are co-circular.

Lemma 10.1 (Flow). *For any regular point $x \in \mathbb{R}^3$ let $r(x)$ be the driver of x. The steepest ascent of the distance function d at x is in the direction of $x - r(x)$.*

Proof. Let $v(x)$ be the vector along which d increases the most at x. Without loss of generality assume $v(x)$ is a unit vector. Let p be any point in $A(x)$. Let $d_p(x) = d(x, p)^2$. The directional derivative of $d_p(x)$ along $v(x)$ is given by $v(x)^T(x - p) = \|x - p\| \cos\theta_p$ where θ_p is the angle between $v(x)$ and $\mathbf{x}_p = x - p$. Since x is regular, $x \notin H(x)$ and thus $0 \leq \theta_p < \pi$. Also, $\|x - p\|$ is same for all $p \in A(x)$. These facts imply that $v(x)$ is along a direction that minimizes the maximum of the angles θ_p over all $p \in A(x)$. The negated vector, $-v(x)$, is along the direction which minimizes the maximum of the angles made by $-v(x)$ and vectors $-\mathbf{x}_p$ for each $p \in A(x)$.

Consider the ball $B = B_{x,d(x)}$. The ball B contains all points of $A(x)$ on its boundary. Let the ray of $-v(x)$ intersect the boundary of B at v'. Normalizing B to a unit sphere, the angle θ_p is given by the length of the spherical arc $v'p$. Therefore, v' minimizes the maximum spherical arc distances $v'p$ to each $p \in A(x)$.

Consider the unbounded polyhedral cone C_x formed by all rays originating from x and going through the points of $H(x)$. The convex hull of any subset $A'(x) \subseteq A(x)$ is projected radially on the boundary of B by this cone. Call this the spherical hull of $A'(x)$. In particular, the polytope $H(x)$ is projected on the boundary of B by this cone. Denote the spherical hull of $H(x)$ with $H'(x)$. Notice that the vertex set of $H(x)$ and $H'(x)$ is the same. From our previous discussion, it is clear that v' has to lie within $H'(x)$ to minimize the maximum arc distances to the vertices of $H'(x)$. Let the minmax distance of v' from the vertices of $H'(x)$ be realized by a subset $A'(x) \subseteq A(x)$ of vertices. We claim that v' lies on the spherical hull of $A'(x)$. If not, v' can be moved ever slightly to decrease the minmax distance. This means the ray of $-v(x)$

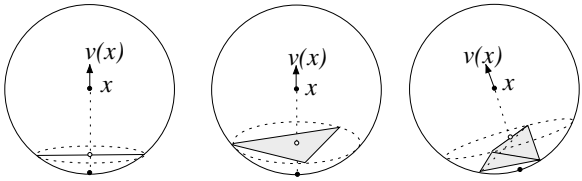

(a) (b) (c)

Figure 10.3. The vector $v(x)$ for one-, two-, and three-dimensional $H(x)$ is shown (from left to right). The hollow circle on $H(x)$ is the driver $r(x)$.

intersects the convex hull of $A'(x)$, say at z, where z is the center of the smallest disk circumscribing the vertices of $A'(x)$.

We claim that z is the closest point of $H(x)$ to x, that is, $z = r(x)$ and $v(x)$ is along the direction $x - r(x)$ as z lies on the ray $-v(x)$.

The spherical disk centering v' and with the vertices of $A'(x)$ on the boundary contains all other vertices of $A(x)$ inside. This means that the smallest (Euclidean) disk, say D, circumscribing the vertices of $A'(x)$ contains all other points of $A(x)$ (if any) on the side that does not contain x. Then, each point of $H(x)$ lies either on D or on the side of D which does not contain x. The center z of D is the closest point to x among all such points. ■

The convex hull $H(x)$ can be zero-, one-, two-, and three-dimensional. Let us look at the Flow Lemma 10.1 for these different cases of $H(x)$ where $x \notin H(x)$.

(i) $H(x)$ is a single point p. In this case trivially $r(x) = p$.
(ii) $H(x)$ is one-dimensional, that is, $A(x) = \{p, q\}$. In this case $r(x)$ is the midpoint of the segment pq [Figure 10.3(a)].
(iii) $H(x)$ is two-dimensional. Consider the disk containing the points of $A(x)$ on the boundary. Let z be the center of this disk. If z is contained in $H(x)$, then $r(x) = z$ (Figure 10.3(b)). If z lies outside $H(x)$, then the midpoint of the edge of $H(x)$ which is closest to x is $r(x)$.
(iv) $H(x)$ is three-dimensional. The closest point to x on the boundary of $H(x)$ is $r(x)$. It is the circumcenter of either a facet or an edge of $H(x)$ (Figure 10.3(c)).

10.2.2 Discrete Flow

The Flow Lemma 10.1 prompts us to define a vector field $v\colon \mathbb{R}^3 \to \mathbb{R}^3$ as

$$v(x) = \frac{x - r(x)}{\|x - r(x)\|} \text{ if } x \neq r(x) \text{ and } 0 \text{ otherwise.}$$

Note that the vector field vanishes exactly at the critical points since $x \neq r(x)$ holds for all regular points. The flow induced by the vector field v is a function $\phi : \mathbb{R}^+ \times \mathbb{R}^3 \to \mathbb{R}^3$ such that the right derivative at every point $x \in \mathbb{R}^3$ satisfies the following equation:

$$\lim_{t \downarrow t_0} \frac{\phi(t, x) - \phi(t_0, x)}{t - t_0} = v(\phi(t_0, x)).$$

Notice that here we use $\mathbb{R}^+$ instead of $\mathbb{R}$ for the domain of t. The reason will be clear in a moment.

Let us explain how ϕ varies with t and x to obtain a more intuitive idea. For any critical point x

$$\phi(t, x) = x, \text{ for all } t \in \mathbb{R}$$

since $r(x) = x$ gives $v(x) = 0$. When x is not critical, let R be the ray originating at x and shooting in the direction $x - r(x)$. Let z be the first point on R where $r(z)$ is different from $r(x)$. If z does not exist, replace it by the point p_∞ at infinity. Then, for $t \in [0, \|z - x\|]$,

$$\phi(t, x) = x + t \frac{x - r(x)}{\|x - r(x)\|}.$$

When $t > \|z - x\|$ the flow is

$$\begin{aligned} \phi(t, x) &= \phi(t - \|z - x\| + \|z - x\|, x) \\ &= \phi(t - \|z - x\|, \phi(\|z - x\|, x)). \end{aligned}$$

It can be shown that ϕ has the following properties as in the smooth case:

(i) ϕ is well defined on $\mathbb{R}^+ \times \mathbb{R}^3$
(ii) $\phi(0, x) = x$
(iii) $\phi(t, \phi(s, x)) = \phi(t + s, x)$.

The definition of $\phi(t, x)$ is valid only for positive t. In the discrete case, it may happen that flows overlap. As a result, for a point x there may not be a unique flow curve for negative t. This makes the definition of a flow curve a little more difficult. An open curve $\gamma : \mathbb{R} \to \mathbb{R}^3$ is a *flow curve* originating at a critical point c if the following holds. For any $\epsilon > 0$, there is a point $y \in B_{c,\epsilon}$ so that $\phi(t, y)$ is contained in γ. The critical point $\lim_{t \to \infty} \phi(t, y)$ is called the destination of the flow curve γ.

Our definition implies that the closure of a flow curve is a piecewise linear curve starting and ending at critical points. Each line segment of this flow curve is along the direction determined by any point on the segment and its driver. The flow curve changes the direction precisely at the points where driver changes

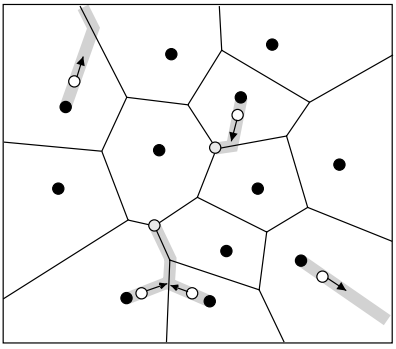

Figure 10.4. Some subsets of the flow curves induced by a set of points in $\mathbb{R}^2$. Flow curves originating at two bottom-most points merge and reach a Voronoi vertex which is a maximum after changing directions twice.

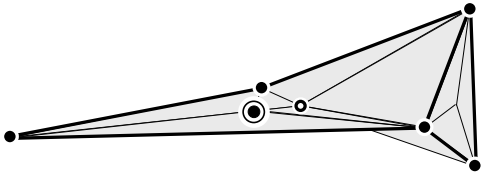

Figure 10.5. An example of an index 2 saddle point (doubly circled) whose stable manifold contains a Voronoi vertex (hollow circle). The points flowing to this Voronoi vertex constitute a three-dimensional region. So, the stable manifold contains both two- and three-dimensional parts. Solid circles are minima, that is, points from P.

(see Figure 10.4). Flow curves may overlap but never cross each other. Also, the Flow Lemma 10.1 implies that, once they overlap they remain so. This is because at each regular point, there is a unique direction along which v is defined. We can now talk about the stable manifolds of the critical points of d. For reconstruction, we will use stable manifolds in Section 10.3. In the sequel, we describe several properties related to the stable manifolds. The readers should observe that they also hold for unstable ones with appropriate modifications.

Just as in the smooth case we look into the regions whose points flow into a critical point of d. Recall that the critical points of d are the fixed points of ϕ. Let c be a critical point of d which means c belongs to the convex hull $H(c)$. The dimension of $H(c)$ is the index of c. The stable manifold $S(c)$ of c is again defined as the space of c and all flow curves with destination c. Let c have index j. We expect that $S(c)$ is j-dimensional. However, it may happen that $S(c)$ has points with neighborhoods homeomorphic to $\mathbb{R}^k$ where $k > j$, (see Figure 10.5). This is attributed to certain kind of nondegeneracies which we eliminate for simpler discussions.

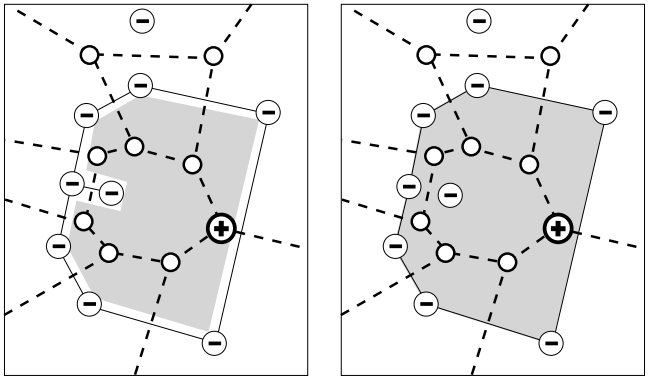

Figure 10.6. The stable manifold $S(c)$ where c is a maximum (marked as $\oplus$) is shaded on the left and $S^*(c)$ is shown on the right. The points of P are minima (marked as $\ominus$). Voronoi vertices are hollow circles.

Nondegeneracy Assumption

For any critical point c, $S(c)$ has no points with k-dimensional neighborhood where $k > j$, the index of c.

We will compute the closures of $S(c)$ in $\mathbb{R}^3$ which we denote as $S^*(c)$. We call $S^*(c)$ the *closed stable manifold* of c. Figure 10.6 illustrates the effect of taking these closures.

10.2.3 Relations to Voronoi/Delaunay Diagrams

The critical points of the distance function d and their stable manifolds associated with the discrete flow are intimately related to the Voronoi and Delaunay diagrams. This enables us to compute them from these diagrams.

Lemma 10.2 (Driver). *Let $x \in \mathbb{R}^3$ be any point and μ be the lowest dimensional Voronoi face in* Vor P *containing x. The driver $r(x)$ is the closest point to x on the Delaunay simplex dual to μ.*

Proof. It follows from the definitions that each point $p \in A(x)$ has x in V_p. This means $\mu = \bigcap_{p \in A(x)} V_p$. Also, Conv $A(x) = H(x)$ is the Delaunay simplex dual to μ by definition. The driver $r(x)$ is the closest point to x in $H(x) =$ dual μ. ■

The following lemma is key in identifying the critical points and their stable manifolds.

Lemma 10.3 (Critical Point). *A point x is critical for the function d if and only if there is a Voronoi face $\mu \in \text{Vor } P$ and its dual Delaunay simplex $\sigma \in \text{Del } P$ so that $x = \sigma \cap \mu$. Also, the index of x is the dimension of σ.*

Proof. If $x = \sigma \cap \mu$, we have $x \in \mu$. For each point $x \in \mu$, $\sigma = \text{dual}\, \mu \subseteq H(x)$. Since $x \in \sigma \subseteq H(x)$, x is critical by definition.

To show the other direction assume that x is critical and μ be the lowest dimensional Voronoi face containing x. By definition of critical points, $x \in H(x)$. Also, by definition, $H(x)$ is the dual Delaunay simplex σ of μ. Therefore, $x \in \sigma \cap \mu$.

The index of x is the dimension of $H(x) = \sigma$. ■

We can make the following observations about the stable manifolds of different types of critical points.

Index **0** *Critical Points*

These are the points of P which are local minima of the distance function d. They can also be thought of as intersections among Voronoi cells and their dual Delaunay vertices. The stable manifolds of these points are the points themselves.

Index **1** *Critical Points*

These are the critical points where a Delaunay edge intersects its dual Voronoi face. The interior of the Delaunay edge is the stable manifold of the corresponding critical point. These types of critical points are also called *saddles* of index 1. Recall that the Delaunay edges that intersect their dual Voronoi face (facet in three dimensions) are called Gabriel edges. Therefore, the closed stable manifolds of index 1 saddles are comprised of the Gabriel graph.

Index **2** *Critical Points*

These critical points are also called index 2 *saddles*. These are the points where a Delaunay triangle intersects its dual Voronoi edge. The stable manifold of such a saddle point is a piecewise linear surface bounded by the stable manifolds of the index 1 saddles together with the minima which are nothing but Gabriel edges. The stable manifolds of index 2 saddles play a vital role in the surface reconstruction procedure described in Section 10.3.

Index **3** *Critical Points*

These are the maxima of d. They are the Voronoi vertices contained in their dual Delaunay tetrahedra. The stable manifolds of these maxima are the

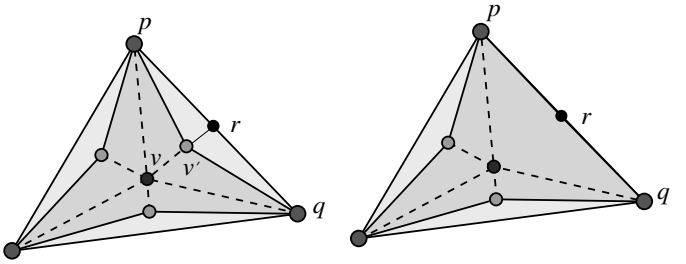

Figure 10.7. Construction of $S^*(c)$ when $v = c$. In the left picture pq is not Gabriel. In the right picture, pq is Gabriel.

three-dimensional cells bounded by the stable manifolds of index 2 saddles and their boundaries.

10.3 Reconstruction with Flow Complex

The surface reconstruction that we are about to describe uses the closed stable manifolds of the index 2 saddles. These stable manifolds are simplicial 2-complexes which decompose $\mathbb{R}^3$ into chambers, the stable manifolds of the maxima. This simplicial 2-complex is called the *flow complex* for P. The closed stable manifolds of index 2 saddles are best described procedurally which also leads to an algorithm to compute them.

10.3.1 Flow Complex Construction

Let c be an index 2 saddle. We will build $S^*(c)$ incrementally. At any generic step, it is a simplicial 2-complex where the vertices are points from P, the midpoints of the Gabriel edges, and some other points on the Voronoi edges. The boundary of $S^*(c)$ lies on the Gabriel edges. Let v be any vertex on the boundary of the 2-complex constructed so far where v is on a Voronoi edge e. Assuming general positions, e has three Voronoi facets incident on it. For each such facet μ, one or two triangles with its edges and vertices are added to the complex. Let $pq = \text{dual}\,\mu$ be the dual Delaunay edge of μ. Let r be the midpoint of the edge pq. If pq is a Gabriel edge, add the triangle pvq to $S^*(c)$, see the picture on right in Figure 10.7. Otherwise, the driver of the interior points of μ is r. In that case let v' be the point where the ray from r to v intersects μ for the first time. Add the triangles pvv' and qvv' with their edges and vertices to the 2-complex $S^*(c)$. See the picture on left in Figure 10.7. The process goes on as long as there is a point v on the boundary of the constructed

2-complex which is on a Voronoi edge. The above construction of $S^*(c)$ starts with $v = c$ and the Voronoi edge e containing c.

```
FlowComplex(P)
 1  T:=∅;
 2  compute Vor P and Del P;
 3  compute the set C of index 2 saddles;
 4  for each c ∈ C do
 5    σ:= Delaunay triangle containing c;
 6    for each Delaunay edge e incident to σ do
 7      push (c, e) into stack S;
 8    endfor
 9    while S ≠ ∅ do
10      (v, e):= pop S;
11      mark e processed;
12      p, q:= endpoints of e;
13      if e contains a saddle of index 1
14        T:=T ∪ {pvq};
15      else
16        μ:= dual e;
17        r:= driver of the interior of μ;
18        v′:= the first point r→v intersects μ;
19        T:= T ∪ {vv′p, vv′q};
20        σ′:= Delaunay triangle dual to the Voronoi edge containing v′;
21        for each edge e′ ≠ e incident to σ′ do
22          if (e′ not processed) push (v′, e′) into S;
23        endfor
24      endif
25    endwhile
26  endfor
27  output Fl P:= 2-complex made by T.
```

10.3.2 Merging

The flow complex Fl P decomposes $\mathbb{R}^3$ into cells which are the closed stable manifolds of the maxima including the maximum p_∞ at infinity. We merge these cells in order to get a manifold surface.

We know that the closed stable manifolds have recursive structures in the sense that a closed stable manifold of index j critical point has the closed stable manifolds of the index $j-1$ critical points on its boundary. We use this

recursive structure of closed stable manifolds for merging. Let a and b be two maxima where $S^*(a)$ and $S^*(b)$ share a closed stable manifold $S^*(c)$ of an index 2 saddle. Merging a and b means to remove $S^*(c)$ from the flow complex $\mathrm{Fl}\, P$. Of course it is not appropriate to merge maxima in arbitrary order nor does it make sense to merge every pair of adjacent maxima.

The order in which the pairs of maxima are merged is determined as follows. Let a and b be a pair with $S^*(c)$ on the common boundary of $S^*(a)$ and $S^*(b)$. Associate the value $\max\{d(a) - d(c), d(b) - d(c)\}$ with the pair (a, b) as its weight. The weight of a pair signifies how deep the maxima are relative to the boundary shared by their closed stable manifolds. Deep maxima capture the shape represented by P more significantly. Therefore, the merging process merges the pairs of maxima in the increasing order of their weights up to a threshold. The 2-complex resulting from the merging process is output. Clearly, this reconstruction depends on the user supplied threshold. The choice of a threshold is not easy in practice. Heuristics such as enforcing a topological disk neighborhood for each sample point while eroding the flow complex may be used to improve the output quality.

10.3.3 Critical Point Separation

The difficulty in merging the cells in the flow complex can be bypassed with a different approach that exploits the *separation* property of the critical points. This property says that the critical points are of two categories, ones that stay near the surface and the other ones that stay near the medial axis. This property holds when the sample P is sufficiently dense for a surface Σ. As before, we will assume Σ is compact, connected, C^2-smooth, and without boundary. Let M denote its medial axis.

Recall that, for a point $x \in \mathbb{R}^3 \setminus M$, $\tilde{x}$ denotes its closest point in Σ. Consider the medial ball at $\tilde{x}$ on the side of Σ as x is. Let $\rho(x)$ and $m(x)$ be the radius and the center of this medial ball. The following lemma states the separation property of the critical points. We will skip the proof (Exercise 5).

Lemma 10.4 (Separation). *Let d be the distance function defined for a ε-sample P of Σ where $\varepsilon \leq \frac{1}{3}$. A point $x \in \mathbb{R}^3 \setminus M$ is critical for d only if $\|x - \tilde{x}\| \leq \varepsilon^2 f(\tilde{x})$ or $\|x - m(x)\| \leq 2\varepsilon\rho(x)$.*

Motivated by the Separation Lemma 10.4, we call a critical point c of d *surface critical* if $\|c - \tilde{c}\| \leq \varepsilon^2 f(\tilde{c})$ and *medial axis critical* otherwise. Since a medial axis critical point c is far away from the surface, the vector $\overrightarrow{pc}$ from its closest sample point p makes a small angle with the normal $\mathbf{n}_p$ (Normal

Lemma 3.2) and hence with the pole vector $\mathbf{v}_p$. On the other hand, a surface critical point c being close to the surface makes the vector $\overrightarrow{pc}$ almost parallel to the surface (Exercise 5). This becomes the basis of the algorithm for separating the two types of the critical points.

Lemma 10.5 (Angle Separation). *Let c be a critical point of d and $p \in P$ be a sample point closest to c. For $\varepsilon \leq 0.1$, the angle $\angle_a(\overrightarrow{pc}, \mathbf{v}_p)$ is at least 75.5° if c is surface critical and is at most 28° if c is medial axis critical.*

The Angle Separation Lemma 10.5 motivates the following algorithm.

```
SEPARATE(Vor P,C)
1  for each p ∈ P do
2    for all critical points c ∈ C in V_p do
3      if ∠_a(pc, v_p) < π/4
4        label c surface critical;
5      else
6        label c medial axis critical;
7      endif
8    endfor
9  endfor.
```

Once the critical points are separated, one can take the closed stable manifolds of the medial axis critical points and produce the boundary of their union. Of course, one has to differentiate the critical points residing near the *inner* medial axis from those near the *outer* one. The boundary of $\bigcup S^*(c)$ approximates the surface where c is taken over any one of these two classes. We use a union-find data structure U on the set of medial axis critical points to collect either all inner medial axis critical points or the outer ones. Suppose c is a maximum near the inner medial axis. The boundary of $S^*(c)$ has the stable manifolds of index 1 and index 2 saddles. If any of these saddles are medial axis critical, we collect them in the same group using the union-find data structure.

The routine CRITSEP returns all outer medial axis critical points.

```
CRITSEP(Vor P)
1  compute the set of critical points C;
2  SEPARATE(Vor P, C);
3  let C_M be the set of medial axis critical points
     including p_∞;
4  initialize a union-find data structure U with all c ∈ C_M;
5  for each c ∈ C_M do
```

```
6     for all c' ∈ (bd S*(c)) ∩ C_M do
7       U.union(c, c');
8     endfor
9   endfor
10  return the component of the union containing p_∞.
```

Once all outer medial axis critical points are collected, one can output the boundary of the union of their closed stable manifolds as the output surface.

SmRecon(P)
1 compute Vor P;
2 C:=CritSep(Vor P);
3 output bd $(\bigcup_{c\in C} S^*(c))$.

It can be proved that the output of SmRecon is homeomorphic to Σ if P is sufficiently dense and is locally uniform (Exercise 6).

10.4 Reconstruction with a Delaunay Subcomplex

The flow complex computes the stable manifolds for the index 2 saddles exactly from the Delaunay triangulation. Since these stable manifolds are not necessarily a subcomplex of the Delaunay triangulation, the output surface triangles are not necessarily Delaunay. The exact complexity of the flow complex is not known. Certainly, it introduces extra points in the output other than the input ones. However, it is not clear if the number of extra vertices could be too many. Also, computing the triangles for the index 2 saddles is somewhat cumbersome. From a practical viewpoint it is much simpler and sometimes desirable to compute the output as a Delaunay subcomplex. In this section we describe an algorithm called Wrap that computes the output surface as a Delaunay subcomplex. The Morse theoretic framework used for the flow complex remains the same though some different interpretations are needed.

10.4.1 Distance from Delaunay Balls

We will use a different distance function in this section. A Delaunay ball $B_{c,r}$ is treated as a weighted point $\hat{c} = (c, r)$. Recall from Section 6.1 that the power distance of a point x from a weighted point $\hat{c}$ is

$$\pi(x, \hat{c}) = \|x - c\|^2 - r^2.$$

For a point set $P \subset \mathbb{R}^3$, let C denote the centers of the Delaunay balls in Del P and $\hat{C}$ denote the set of weighted points corresponding to these Delaunay balls.

These Delaunay balls also include the ones that circumscribe the infinite tetrahedra in Del P. These infinite tetrahedra are formed by a convex hull triangle together with the point p_∞. Obviously, their centers are at infinity and they have infinite radii. Define a distance function $g : \mathbb{R}^3 \to \mathbb{R}$ as

$$g(x) = \min_{\hat{c} \in \hat{C}} \pi(x, \hat{c}).$$

Recall from Section 6.1 that the power diagram Pow $\hat{C}$ is the decomposition of $\mathbb{R}^3$ into cells and their faces determined by the power distance. When the weighted points are the centers of the Delaunay balls with their radii as weights, the power diagram coincides with the Delaunay triangulation. This means Pow $\hat{C}$ = Del P (Exercise 9). So, if a point $x \in \mathbb{R}^3$ lies in a Delaunay tetrahedron $\sigma \in$ Del P, $g(x)$ is exactly equal to $\pi(x, \hat{c})$ where c is the center of the Delaunay ball of σ. The distance function g is continuous but not smooth. The nonsmoothness occurs at the triangle, edges, and vertices of the Delaunay tetrahedra. Notice that the minima of this distance function occur at the centers of the Delaunay balls which are the Voronoi vertices. Not all Voronoi vertices but only the ones contained in their dual Delaunay tetrahedra are minima. The function g is negative everywhere except at the Delaunay vertices, that is, at the points of P. The points of P reside on the boundary of the Delaunay balls and thus have the value of g as zero. They become the maxima of the distance function g.

Similar to the distance function d defined in Section 10.2, we can introduce a flow induced by g. This calls for the notion of driver for each point under the function g.

Definition 10.3. *For every point $x \in \mathbb{R}^3$, let $H(x)$ be the convex hull of the points in C with the minimum power distance to x. The driver $r(x)$ of x is defined as the point in $H(x)$ closest to x. The point x is* critical *if $x \in H(x)$ and is* regular *otherwise.*

We have a counterpart of the Flow Lemma 10.1 for g.

Lemma 10.6 (Second Flow Lemma). *For any regular point $x \in \mathbb{R}^3$ the steepest ascent of g at x is in the direction of $x - r(x)$.*

We have a vector field $v : \mathbb{R}^3 \to \mathbb{R}^3$ as before defined by the steepest ascent direction of g and a flow $\phi : \mathbb{R}^+ \times \mathbb{R}^3 \to \mathbb{R}^3$ induced by it. Again, the flow curves derived from ϕ are piecewise linear curves and these flow curves have the property that they are either disjoint or overlap, but they never cross each other. Also, the Second Flow Lemma 10.6 implies that, once they join together

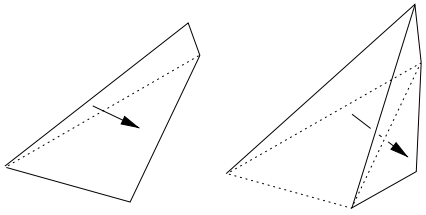

Figure 10.8. The dotted simplex is σ, an edge on the left, and a triangle on the right. The black arrow shows the flow direction from predecessor τ toward the successor ξ of σ.

they remain so. To be consistent with the smooth case we will denote a flow curve passing through a point x as ϕ_x.

The minima of g occur at a subset of Voronoi vertices. We are interested in the unstable manifold of these minima. In particular, we compute an approximation of the closed unstable manifold $U^*(p_\infty) = \mathrm{Cl}\, U(p_\infty)$ of the minimum p_∞. The boundary of this approximation is the reconstructed surface. In general, this boundary is a subcomplex of Del P which we refer as the *wrap complex*.

10.4.2 Classifying and Ordering Simplices

The flow curves lead to an acyclic relation over the set of Delaunay simplices. The wrap complex is constructed by collapsing simplices following the order induced by this relation.

Flow Relation

Assume a dummy simplex σ_∞ that represents the outside, or the complement of Conv P. It replaces all infinite tetrahedra formed by the convex hull triangles and the point p_∞. All these tetrahedra have similar flow behavior and can be treated uniformly. Let $D = \mathrm{Del}\, P \cup \{\sigma_\infty\}$. The flow relation $\prec$ on D mimics the behavior of the flow curves.

Definition 10.4. *We say $\tau \prec \sigma \prec \xi$ if σ is a proper face of τ and of ξ and there is a point $x \in \mathrm{Int}\,\sigma$ with ϕ_x passing from $\mathrm{Int}\,\tau$ through x to $\mathrm{Int}\,\xi$. We refer this as τ precedes σ and σ precedes ξ. The condition implies that every neighborhood of x contains a nonempty subset of $\phi_x \cap \mathrm{Int}\,\tau$ and a nonempty subset of $\phi_x \cap \mathrm{Int}\,\xi$. We call τ a* predecessor *and ξ a* successor *of σ.*

Notice that predecessor successor relations are defined for σ. It is not true that if τ is a predecessor (successor) of σ, then σ is a successor (predecessor) of τ.

Figure 10.8 illustrates the predecessor and successor relation for an edge and a triangle. Based on the relation $\prec$ we also define the *descendents* and *ancestors*

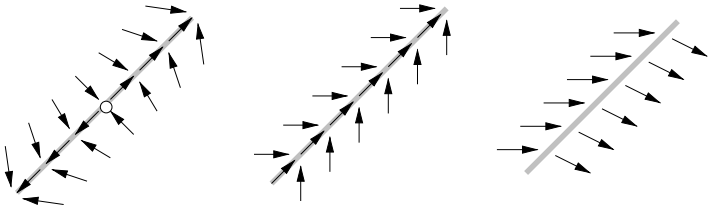

Figure 10.9. Different types of flow through edges.

of a simplex. Basically, the descendents of a simplex are a set of simplices that can be reached from σ by transitive closure of $\prec$. The ancestors are the simplices which can reach σ by transitive closure of $\prec$.

Definition 10.5. *For a simplex σ, the descendents,* $\operatorname{Des}\sigma$*, are defined as*

$$\operatorname{Des}\sigma = \{\sigma\} \cup \bigcup_{\sigma \prec \xi} \operatorname{Des}\xi.$$

The ancestors, $\operatorname{Anc}\sigma$*, are defined as*

$$\operatorname{Anc}\sigma = \{\sigma\} \cup \bigcup_{\tau \prec \sigma} \operatorname{Anc}\tau.$$

The flow curves intersect the Delaunay simplices either in intervals or in single points. Any point x in the interior of a Delaunay simplex σ has the Voronoi face $\operatorname{dual}\sigma$ as $H(x)$. Therefore, all interior points in σ have the same driver $r(x)$. This means that the intersections of all flow curves with the interior of a Delaunay simplex are similar, that is, either all of them are points, or all of them are intervals. According to the pattern of these intersections and associated flows we classify the Delaunay simplices into three categories. The three categories are mutually exclusive and exhaust all possible Delaunay simplices.

Centered Simplices

A simplex $\sigma \in \operatorname{Del} P$ is *centered* if and only if its interior intersects the interior of the dual Voronoi face $\mu = \operatorname{dual}\sigma$. The intersection point $y = \operatorname{Int}\sigma \cap \operatorname{Int}\mu$ is a critical point and its index is the dimension of μ. The flow curves intersecting centered simplices have the property that the portion of ϕ_x succeeding $x \in \operatorname{Int}\sigma$ is contained in $\operatorname{Int}\sigma$. Consequently, centered simplices do not have any predecessor or successor. The leftmost edge of Figure 10.9 and the leftmost triangle in Figure 10.10 are centered.

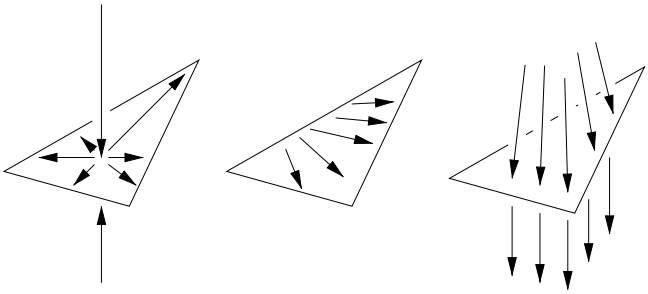

Figure 10.10. Different flow types for triangles.

Confident Simplices

A simplex $\sigma \in \text{Del}\, P$ is *confident* if and only if it is not centered and its affine hull intersects the interior of $\mu = \text{dual}\, \sigma$. Confident simplices are similar to the centered ones, in the sense that they would be centered if they covered large enough portion of their affine hulls. The neighborhoods of the flow curves succeeding any interior point of a confident simplex remain in the interior of the simplex. The edge in the middle of Figure 10.9 and the middle triangle in Figure 10.10 are confident.

All simplices that have a confident simplex σ as a predecessor or successor are faces of σ. We call them predecessor and successor faces of σ. The successor faces can be determined as follows. Let $z = \text{aff}\, \sigma \cap \text{Int}\, \mu$. The point z is the center of the smallest ball circumscribing σ. Let $k = \dim \sigma$. Consider each $(k-1)$-dimensional face ξ of σ. The $\text{aff}\, \xi$ either separates z from the interior of σ or both z and $\text{Int}\, \sigma$ lie on the same side of $\text{aff}\, \xi$. We assume here the general positions which preclude z lying on $\text{aff}\, \xi$. A face ξ of σ is a predecessor if and only if the affine hulls of all $(k-1)$-dimensional faces containing ξ separate z from the interior of σ. Each confident simplex has a unique lowest dimensional predecessor face v contained in all predecessor faces of σ.

Equivocal Simplices

A simplex $\sigma \in \text{Del}\, P$ is *equivocal* if and only if its affine hull does not intersect the interior of the dual Voronoi face $\mu = \text{dual}\, \sigma$. The flow curves intersect equivocal simplices in a single point. The rightmost edge of Figure 10.9 and the rightmost triangle in Figure 10.10 are equivocal.

All predecessors and successors of an equivocal simplex σ are cofaces of σ. They are either centered or confident. An equivocal simplex can have more than one predecessors but only one successor.

Lemma 10.7 (Successor Lemma). *Each equivocal simplex has exactly one successor.*

Proof. Let σ be an equivocal simplex and $x \in \operatorname{Int}\sigma$. Consider the flow curves passing through x. Because of the Second Flow Lemma 10.6, we know that all flow curves leave x along the same direction. Since after x all flow curves are the same in a sufficiently small neighborhood, consider the flow curve ϕ_x and a small portion immediately succeeding x. This portion is a line segment contained in the interior of a simplex ξ where $\sigma \prec \xi$. The simplex ξ is confident. Every flow curve that intersects ξ does so in a portion of a line passing through the center z of the smallest ball circumscribing ξ. It follows that for each point $x \in \sigma$, a sufficiently small portion of ϕ_x succeeding x lies on the line joining x and z and therefore in $\operatorname{Int}\xi$. This implies that each x identifies the same simplex ξ which becomes the only successor of σ. ■

The successor ξ of σ can be computed as follows. Let μ be the dual Voronoi face of σ. The closest point of μ to ξ is z which resides on the boundary of μ. Testing over all boundary Voronoi faces of μ, the Voronoi face μ' containing z can be determined. The successor ξ is the dual Delaunay simplex of μ'.

10.4.3 Reconstruction

The basic construction of the WRAP algorithm computes a subcomplex $\mathcal{X}$ from Del P whose boundary is output as the wrap surface $\mathcal{W}$. In general this surface is homotopy equivalent to $\mathbb{S}^2$ though other topologies can be accommodated with some postprocessing. It is constructed by peeling away simplices dictated by the flow relation.

A *source* is a simplex $\sigma \in$ Del P without any predecessor in the flow relation. The sources are exactly the centered simplices including σ_∞. We are interested in computing an approximation of the closed unstable manifold of p_∞. This approximation is obtained by following the flow relation. A very important property of the flow relation is that it is acyclic. A *cycle* is a sequence of simplices $\sigma_1 \prec \sigma_2 \prec \cdots \prec \sigma_\ell$, with $\ell \geq 3$ and $\sigma_1 = \sigma_\ell$.

Lemma 10.8 (Acyclicity). *The flow relation $\prec$ is acyclic.*

Proof. Let $\sigma_i \in$ Del P and $B_i = B_{c_i, r_i}$ be the smallest empty ball circumscribing σ_i. Consider $\sigma_i \prec \sigma_j$. Clearly, σ_j cannot be centered. If σ_j is confident then σ_i is equivocal and we have $B_i = B_j$ and $\dim\sigma_i < \dim\sigma_j$. If σ_j is equivocal then σ_i is centered or confident. Hence, $c_i \neq c_j$ and $r_i^2 > r_j^2$. We assign to each σ_i

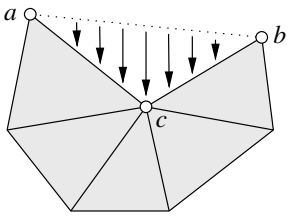

Figure 10.11. Collapsing an edge triangle pair.

the pair $(r_i^2, -\dim \sigma_i)$. The pairs decrease lexicographically along the chain preventing a cycle in it. ■

The sources and their descendent sets are analogous to the critical points and their unstable manifolds respectively. However, they are not exactly same. Approximations of the unstable manifolds with Delaunay subcomplexes face a difficulty with simplices that have more than one predecessor. Their existence causes possible overlap of the descendent sets. This is in contrast with the unstable manifolds of smooth functions which are necessarily disjoint though their closures may overlap. Equivocal edges may have more than one predecessor. Similarly, confident tetrahedra may have more than one predecessor face. Despite the possibility of overlapping descendent sets, a useful containment property for unstable manifolds holds. Let σ and τ be the centered simplices with the critical points $y \in \operatorname{Int} \sigma$ and $z \in \operatorname{Int} \tau$.

Lemma 10.9 (Descendent). $U(z) \subseteq \operatorname{Cl} U(y)$ *implies* $\operatorname{Des} \tau \subseteq \operatorname{Cl} \operatorname{Des} \sigma$.

The set $\mathcal{X}$ whose boundary is output as the wrapping surface is constructed from $\operatorname{Del} P$ by taking out a conservative subset of $\operatorname{Des} \sigma_\infty$. The simplices in $\operatorname{Des} \sigma_\infty$ which have more than one predecessor are eliminated to define the conservative descendent subset. By looking at the complement, we can say that $\mathcal{X}$ is exactly equal to the union of the descendent sets of all sources except that of σ_∞. In other words, the wrapping surface $\mathcal{W}$ is the boundary of

$$\mathcal{X} = \bigcup_{\text{sources } \sigma \neq \sigma_\infty} \operatorname{Des} \sigma.$$

10.4.4 Algorithm

The algorithm for constructing $\mathcal{W}$ removes simplices from $\operatorname{Del} P$ using collapses (see Figure 10.11). Let $\mathcal{K}$ be a simplicial complex and let σ be a simplex with exactly one proper coface $\tau \in \mathcal{K}$. The removal of the pair (σ, τ) from

$\mathcal{K}$ is called an *elementary collapse*. It is known that the underlying space of $\mathcal{K}_1 = \mathcal{K} \setminus \{\sigma, \tau\}$ is homotopy equivalent to that of $\mathcal{K}$.

An ℓ-simplex σ is *free* if there is a k-simplex τ in $\mathcal{K}$ with $k > \ell$ so that all cofaces of σ are faces of τ. The collapses shrink a subcomplex $\mathcal{Y}$ starting from the full Delaunay complex Del P. Call a simplex σ *collapsible* if

(i) $\sigma \in \mathcal{Y}$ is free and equivocal and
(ii) τ is the highest dimensional coface of σ in $\mathcal{Y}$ where $\sigma \prec \tau$ and σ is the lowest dimensional predecessor face of τ.

A *free collapse* is an operation where a collapsible simplex is removed together with its cofaces. Observe that a free collapse can be implemented with a sequence of elementary collapses. The following algorithm COLLAPSE carries out a sequence of free collapses on a given simplicial complex $\mathcal{Y} \subseteq$ Del P as long as there are collapsible simplices.

COLLAPSE ($\mathcal{Y}$,σ)

```
1  for each face τ of σ do
2    push τ into stack S;
3  endfor
4  while S ≠ ∅ do
5    σ := pop S;
6    if σ collapsible
7      for each coface ξ of σ do
8        Y := Y \ ξ;
9      endfor
10     Let τ be the highest dimensional coface of σ;
11     for each face ξ of τ that is not a coface of σ do
12       push ξ into S;
13     endfor
14   endif
15 endwhile
16 return Y.
```

The algorithm WRAP uses the COLLAPSE routine on the Delaunay triangulation Del P. It starts the collapse with the faces of σ_∞ which are the simplices on the convex hull of P.

WRAP(P)

```
1  compute Del P;
2  output COLLAPSE(Del P, σ∞).
```

The following theorem asserts that no matter which free collapses are chosen among many, the final output $\mathcal{Y}$ of WRAP is actually $\mathcal{X}$.

Theorem 10.1. WRAP *outputs* $\mathcal{X}$.

The output $\mathcal{X}$ of WRAP is obtained from the Delaunay complex Del P through elementary collapses. Since each elementary collapse maintains the homotopy type, the underlying space $|\mathcal{X}|$ of $\mathcal{X}$ is homotopy equivalent to that of Del P and hence to a ball. Notice that $|\mathcal{X}|$ may not be homeomorphic to a three-dimensional ball though is homotopy equivalent to it. In case $|\mathcal{X}|$ is a ball, its boundary is homeomorphic to a sphere. This means that the basic construction of WRAP can reconstruct surfaces that are topologically 2-spheres. To accommodate other topologies, the basic construction needs some modifications.

The idea is to collapse simplices not only from the descendent set of σ_∞ but also from the descendent sets of other significant sources. For a source σ define its size $|\sigma|$ by the value $|g(y)|$ where $y \in \sigma$ is the corresponding critical point of the centered simplex σ. By definition, $g(y)$ is the negated squared radius of the diametric ball of σ. It is intuitive that large sizes of sources indicate the space through which the wrapping surface should be pushed. Keeping this in mind, we sort the sources in order of decreasing size $|\sigma_0| > |\sigma_1| > \cdots > |\sigma_m|$, where $\sigma_0 = \sigma_\infty$ and thus $|\sigma_0| = \infty$. For each index $0 \leq j \leq m$, define

$$\mathcal{X}_j = \bigcup_{i=j+1}^{m} \text{Cl Des}\, \sigma_i.$$

Define $\mathcal{W}_j = \text{bd}\, |\mathcal{X}_j|$. The $\mathcal{X}_j$ form a nested sequence of subcomplexes

$$\mathcal{X} = \mathcal{X}_0 \supseteq \mathcal{X}_1 \supseteq \cdots \supseteq \mathcal{X}_m = \emptyset.$$

Correspondingly, the $\mathcal{W}_j$ form a nested sequence of wrapping surfaces. The operation that removes a principal simplex from a simplicial complex $\mathcal{K}$ is called *deletion*. In contrast to a collapse, a deletion changes the homotopy type of $|\mathcal{K}|$. A particular $\mathcal{X}_j$ is constructed from Del P by a series of deletions and collapses. A source is deleted which is followed by a sequence of collapses taking out all simplices in the descendent set of the source. The complex $\mathcal{X}_j$ is computed by repeating these two operations $j + 1$ times, once for each of $\sigma_0, \sigma_1, \ldots, \sigma_j$.

Alternatively, one may resort to the separation property of the critical points as in Subsection 10.3.3. The distance functions d and g have the same set of critical points (Exercise 11). Therefore, we can use CRITSEP routine to obtain the set of outer medial axis critical points. All sources (Voronoi vertices) in this filtered set can trigger a deletion of its dual tetrahedron and a series of collapse thereafter.

ModifiedWrap(P)
1 C:=CritSep(P);
2 $\mathcal{Y}$:=Del P;
3 sort sources containing $c \in C$ in decreasing order of size;
4 `for` each source σ in the sorted order
5 $\mathcal{Y}$:= Collapse($\mathcal{Y}, \sigma$);
6 `endfor`
7 `output` $\mathcal{Y}$.

10.5 Notes and Exercises

Morse theory is a widely studied subject in mathematics. Milnor [70] and Guillemin and Pollack [60] are two standard books on the subject. The flow induced by distance functions as described in this chapter is relatively new and can be found in Grove [59]. The connection between Morse theory and the Voronoi diagrams was discovered by Edelsbrunner, Facello, and Liang [45] and Siersma [78] in different contexts.

Morse theoretic reconstruction was first discovered by Edelsbrunner in 1995 though it was not published until 2003 [44] due to propriety rights. In this work Edelsbrunner proposed the Wrap algorithm as described in Section 10.4. To circumvent the problem of nonsmooth vector field, he used the fact that a nonsmooth vector field can be approximated by a smooth one with arbitrary precision. Here we used the concept of driver introduced by Giesen and John [55, 56]. They used drivers to apply the idea of the flow in Grove [59] for distance functions induced by a set of discrete points. The flow complex computation as described in Section 10.3 is taken from this work [56]. The separation of critical points as described in Subsection 10.3.3 was discovered by Dey, Giesen, Ramos, and Sadri [32]. The Separation Lemma 10.4 and the Angle Separation Lemma 10.5 were proved in this paper. We took the leverage of this result to introduce ModifiedWrap.

The idea of computing flow and their approximations through Delaunay subcomplexes was further investigated by Dey, Giesen, and Goswami [31] for shape segmentation and shape matching. The Flow Lemma 10.1 and a preliminary proof of it is included there.

Exercises

1. Let P be a set of points in $\mathbb{R}^2$. Characterize the flow complex Fl P when P is unweighted and weighted.
2. Consider the function d as used for the flow complex. Describe the unstable manifolds of the minima of this function.

3. Design an algorithm to compute the unstable manifolds of the index 2 critical points of d.
4. Consider the function d. Design an algorithm to compute the boundary of the stable manifold of p_∞. How should this boundary be modified to improve the reconstruction?
5. Prove the Separation Lemma 10.4 and the Angle Separation Lemma 10.5 [32].

6^h. Prove that the output of SmRecon is homeomorphic to Σ if P is locally uniform and is sufficiently dense [32].

7^o. Prove or disprove 6 when P is a nonuniform sample.

8^o. Determine the worst case optimal complexity of the flow complex.

9. Let $\hat{C}$ be the weighted points corresponding to the Delaunay balls in Del P. Show that Pow $\hat{C}$ = Del P.
10. Consider the function g used for the wrap complex. Describe the stable manifolds of the maxima of g.
11. Prove that the functions d and g have the same set of critical points.
12. Prove the Descendent Lemma 10.9 [44].
13. Give a proof of the Wrap Theorem 10.1 [44].

14^o. Prove that the output of ModifiedWrap is homeomorphic to Σ if the input P is sufficiently dense for Σ.